UV Resonance Raman Spectroscopy Using a New cw Laser Source: Convenience and Experimental Simplicity

SANFORD A. ASHER,* RICHARD W. BORMETT, X. G. CHEN, DONALD H. LEMMON, NAMJUN CHO, PETE PETERSON, MARCO ARRIGONI, LUIS SPINELLI, and JEFF CANNON

Department of Chemistry, University of Pittsburgh, Pittsburgh, Pennsylvania 15260 (S.A.A., R.W.B., X.G.C., D.H.L., N.C.); and Coherent Laser Group, Division of Coherent Inc., 3210 Porter Drive, Palo Alto, California (P.P., M.A., L.S., J.C.)

A new laser has been developed which generates hundreds of milliWatts of cw UV power below 260 nm. The laser consists of a small-frame Ar^+-ion laser which is intracavity doubled with the use of BBO nonlinear optical crystals. More than 300 mW are available at 244 and 257 nm, while 180, 100, and 30 mW are available at 248, 238, and 228.9 nm, respectively. This laser is an ideal source for UV Raman spectroscopy since it avoids the nonlinear and saturation problems common with the typical pulsed laser excitation sources. It also minimizes thermal sample degradation. We demonstrate the increased spectral signal-to-noise ratios possible due to the ability to focus the cw laser into a small-volume element that can be efficiently imaged into the spectrometer. We demonstrate the ability of this laser to excite Raman spectra of solid samples such as coal-liquid residuals, and point out the utility of the 228.9-nm line for studying aromatic amino acids in proteins. We also demonstrate the ability to selectively study pyrene intercalated into calf thymus DNA.

Index Headings: **Instrumention, emission spectroscopy; Lasers, cw, Ar^+; Raman spectroscopy; Spectroscopic techniques; UV-visible spectroscopy.**

INTRODUCTION

UV resonance Raman spectroscopy (UVRR)[1] offers high selectivity and sensitivity for studying the vibrational spectra of the great majority of all molecules which have electronic absorption bands at wavelengths longer than 180 nm. This group includes essentially all organics with at least one double bond and also includes most inorganic compounds. Excitation into the UV absorption bands of polycyclic aromatic hydrocarbons (PAHs) such as pyrene,[2] for example, enhances the Raman cross section by factors of 10^8, which permits studies of low concentrations of these analytes in complex environments.[3-6] The recent development of instrumentation[7,8] capable of UV excitation in the region between 180 and 300 nm now permits the study of aromatic amino acids in proteins,[9-14] and DNA nucleic acid structural studies.[15] UVRR has also been used to examine the nature of molecular electronic excited states of small molecules;[16-18] for example, UVRR studies of amides have indicated that the amide π^* excited state is twisted.[19-21] The high selectivity and sensitivity of this technique permit important analytical applications. Examples include studies of PAHs in coal-derived liquids[4-6] and in petroleum fractions,[22] as well as the use of UVRR for examining low levels of unsaturation in polymers.[22,23] The utility of UVRR results not only from the resonance enhancement phenomenon but also from the fact that fluorescence interference *within* the Raman spectrum does *not* occur in condensed-phase samples excited below 250 nm;[24] fluorescence interference from impurities is a major impediment for Raman studies utilizing *near*-UV, visible, or near-IR excitation.

The strong resonance enhancement which occurs with UV Raman excitation permits spectral measurements with high signal-to-noise (S/N) ratios; however, the typical S/N ratios remain far below the theoretical limit, mainly because of the optical excitation sampling limitations which result from the typical high-pulse energy flux laser excitation generally used. Until now, UV Raman measurements have utilized frequency-doubled YAG or XeCl excimer lasers[7,13,16] with pulse widths of ~10 ns and repetition rates lower than 300 Hz. These lasers pump near-UV or visible wavelength dye lasers. The pulsed dye laser outputs, which have very high peak powers, are converted into the UV through nonlinear optical processes, such as nonlinear frequency doubling and frequency mixing. The result is completely tunable UV light at relatively low duty cycles with very high peak powers. The laser outputs easily obtained have average powers of tens of milliWatts with peak powers of many megaWatts. Focused, these pulses easily cause dielectric breakdown in any sample. Other nonlinear optical phenomena occur even with more diffuse focusing and lower peak powers to compete with the Raman scattering.[25] At even lower peak powers, Raman saturation phenomena can occur, which depopulates the ground state and creates transient concentrations of excited-state species.[10,19a,25,26] To avoid saturation and nonlinear phenomena, one should obtain pulsed Raman measurements with broad defocused laser beams with pulse energy flux densities of less than 1 mJ/cm^2.

The Raman spectrometers used for these measurements require high resolution and utilize narrow slits, generally 100 to 200 μm in width. Given the large f/number required for the spectrograph stage, only a small portion of the illuminated sample width can be focused into the spectrometer. In order to have an incident energy flux density of less than 1 mJ/cm^2, with an incident average power of 20 mW, less than 1% of the incident laser photons can be utilized in a typical backscattering collection geometry that utilizes a collection optic with a magnification of six, a detector of 2.5-mm height, and a slit width of 200 μm in Raman measurements utilizing the 20-Hz-repetition-rate YAG laser system. Less than 10% can be utilized for the 200-Hz excimer laser for samples such as pyrene[2] and trypto-

Received 9 November 1992.
* Author to whom correspondence should be sent.

0003-7028/93/4705-0628$2.00/0

phan,[25] which have significant excited-state lifetimes and which are susceptible to ground-state depletion.

The advent of the high-repetition-rate excimer laser increased the spectral S/N ratios for resonance Raman measurements; however, the increased maintenance and low laser dye lifetime makes it an expensive laser in cost and reliability.[27] Beneficially, however, the excimer laser has permitted UV Raman studies of species with significant excited-state lifetimes such as tryptophan.[12a] Most recently, other groups[22,28] have developed quasi-continuous-wave UV sources that employ mode-locked YAG lasers which give extremely high repetition rates and are considered quasi cw since they have a duty cycle of almost 0.01, which is much higher than that of the highest-repetition-rate excimer laser system (500 Hz), which has a duty cycle of less than 10^{-5}. These systems give good S/N spectra but are relatively expensive and complex, as are the YAG and excimer systems typically used.

RESULTS AND DISCUSSION

This report describes a new cw UV laser based on an intracavity frequency-doubled Ar^+-ion laser which has the output wavelengths and powers shown in Table I. There are five frequency-doubled lines below 260 nm which are obtained by frequency doubling the strong Ar^+-ion lasing lines in the visible spectral region. As shown in Fig. 1, the laser is constructed around a small-frame Coherent Inc. Innova 300 Ar^+-ion laser system. The output coupler is removed, and a modified optical cavity is constructed in which the intracavity beam waist is focused at the center of a BBO doubling crystal. A dielectric mirror, which is completely reflective in the visible but transmittive in the UV, is used as the output coupler. The frequency-doubled radiation exits mirrors M3 and M4. We utilize the UV output from M4 and convert the elliptical output beam to a circular beam by use of a cylindrical lens. For maximization of the frequency-doubled beam intensity stability and its pointing stability, the temperature of the BBO crystal is thermostatically controlled at a temperature slightly elevated over ambient. In addition, a small portion of the UV beam is split off and monitored by a photocell which maximizes the UV output power both by controlling a signal to the Ar^+-ion laser power supply feedback loop which controls the plasma tube current and by controlling a signal which keeps the laser cavity mirror M2 optimally aligned by use of a servo-controlled actively stabilized optical cavity. The laser output also contains plasma emission lines, and the UV output is dispersed by a Pellin Broca prism over a long (~2 m) pathlength in order to separate and remove the plasma emission lines. It is essential to use a fused-silica Pellin Broca prism rather than a crystalline quartz prism to disperse the nonpolarized plasma lines; the birefringent crystal-

TABLE I. Continuous-wave Ar^+-ion laser wavelengths and output powers.

Wavelength (nm)	Power (mW)
228.9	30
238.3	100
244.0	400
248.3	180
257.3	750
275.4	5
300–305.5	20
333.4	40
333.8	30
335.8	20
351.1	200
351.4	60
363.8	240
454.5	140
457.9	420
465.8	180
472.7	240
476.5	720
488.0	1800
496.5	720
501.7	480
514.5	2400
528.7	420

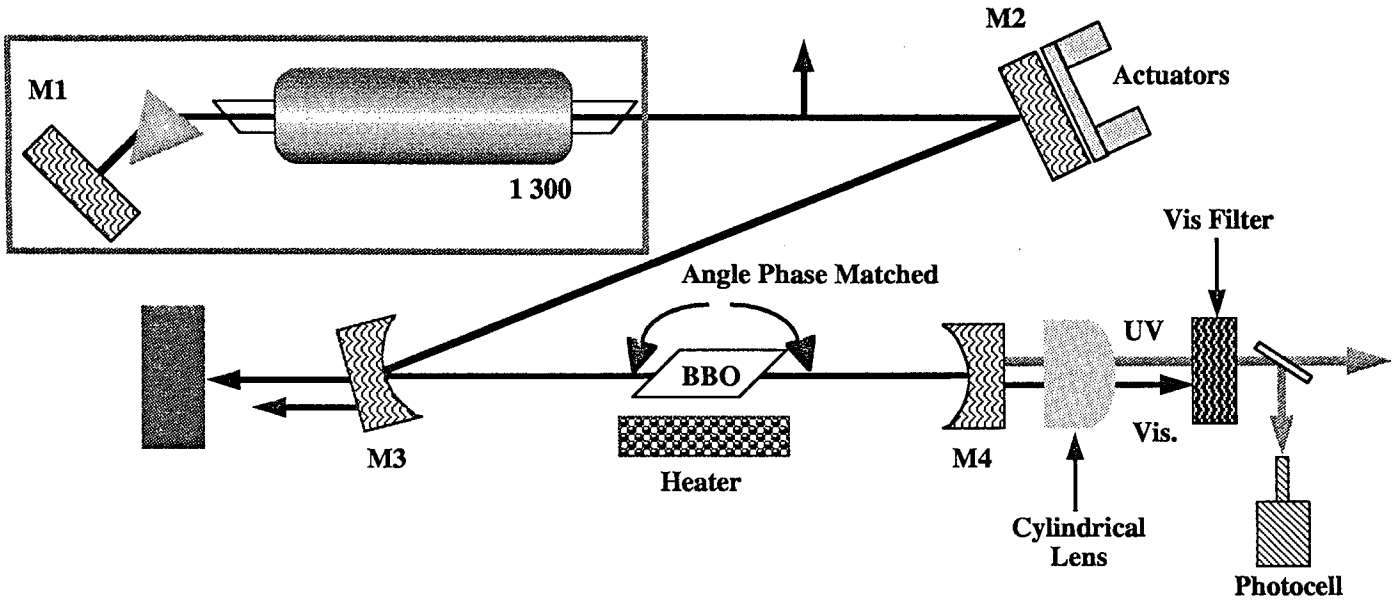

FIG. 1. Diagram showing optical layout of Coherent Innova 300 intracavity frequency-doubled Ar^+-ion laser system.

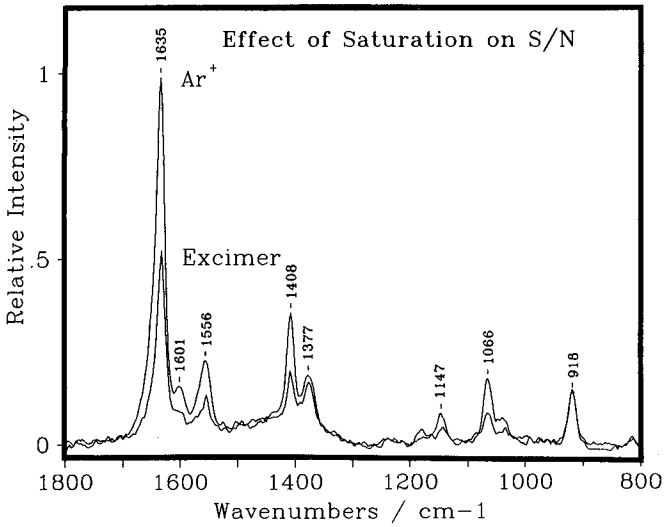

FIG. 2. Raman spectra excited at 244 nm of a 20-μM solution of pyrene in acetonitrile. Laser beams are focused to a 268-μm spot size (1/e intensity) on the sample. Spectral accumulation, 50 seconds. Spectrograph slit width, 100 μm (11 cm^{-1} spectral bandpass). (Top) cw Ar$^+$-ion laser, average power at sample 0.67 mW. (Middle) 100-Hz excimer laser. Average power at sample 0.57 mW. Sample flow rate ~1 mL/min; sample volume completely exchanged between pulses.

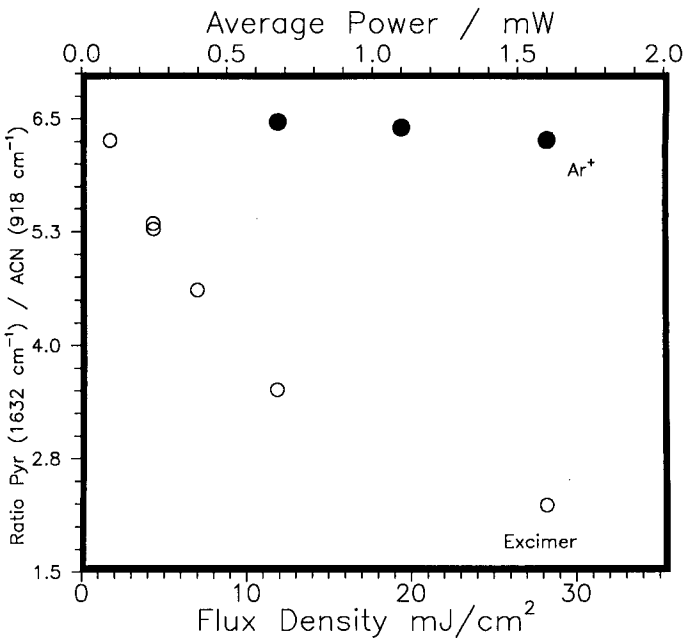

FIG. 3. Raman saturation plot showing the ratio of intensities of the pyrene 1632-cm^{-1} peak to that of the 918-cm^{-1} acetonitrile peak. Open circles show the excimer laser data, while the closed circles show the cw laser data. Conditions are the same as in Fig. 2.

line quartz will overlap the dispersions of the two polarizations and make it difficult to isolate the lasing line.

The frequency-doubled Ar$^+$-ion laser requires careful alignment of the doubling optics when one is tuning between different UV lines, but once tuned and aligned it is indefinitely stable. We expect that the lifetime of the BBO crystals is finite and that they will need to be replaced at regular intervals. We see some damage in the BBO crystals when operated over extended periods of time at the highest powers. However, it appears that we will obtain hundreds of hours of use at the typical powers we are likely to use for spectral measurements.

Figure 2 shows the Raman spectra of pyrene in acetonitrile with 244-nm excitation from both the cw Ar$^+$-ion laser and a 100-Hz-repetition-rate excimer laser system. The spectra were obtained with a 50-s total accumulation time with the use of similar average powers of ~0.6 mW. Both lasers were focused to a ~250-μm spot size. The peaks at 1636 and 592 cm^{-1} derive from the pyrene, while the bands at 918 and 1374 cm^{-1} derive from the acetonitrile solvent. The cw excited spectrum has a higher S/N due to the twofold higher intensity for the pyrene peaks. In contrast, the acetonitrile peak intensities are similar between the spectra. The decreased pyrene intensities relative to the acetonitrile intensities result from Raman saturation, in which the ground-state pyrene concentration is depleted during the pulsed excitation.[7b,25,26] Each excimer pulse delivers 5.7 μJ of energy, which corresponds to 7×10^{12} photons/pulse incident on a sample volume of approximately 5×10^{-5} cc containing 6×10^{11} pyrene molecules, which have long S_1 excited-state lifetimes relative to the laser pulse width. Thus, a significant fraction of the pyrene molecules are transferred up into the S_1 excited state, and the ground-state concentration is depleted.

Figure 3 displays the level of saturation as a function of incident laser energy flux. The plot shows the intensity ratio of a pyrene peak relative to a solvent peak. The pulsed laser saturation plot demonstrates that the pyrene relative intensities can drop by a factor of three for an incident average power value of 1.5 mW, which corresponds to an energy flux value of 26 mJ/cm^2 pulse. In contrast, no saturation should be evident for the cw excitation; 1.5 mW of 244-nm light corresponds to 1.5×10^{15} photons/s. This photon flux is incident on a cylindrical sample volume of 4.9×10^{-5} cc containing 5.9×10^{14} molecules (c = 20 μM); 6% of these photons are absorbed since the molar absorptivity of pyrene in acetonitrile at 244 nm is 13,000/M cm. Given an estimated pyrene S_1 lifetime of 200 ns, less than 10^{-4} of the pyrene molecules should occur in the S_1 excited state under steady-state illumination conditions. However, our observed 6% steady-state pyrene intensity decrease requires an excited-state lifetime of 0.3 ms. This observation may result from the formation of pyrene excimers, which have long lifetimes. In spite of the contribution of excimer excited states, these results clearly demonstrate that cw excitation permits high photon flux excitation and also avoids extensive depletion of the ground-state sample concentration.

The ability to focus the cw Ar$^+$-ion laser to a spot size that can be efficiently imaged into the spectrometer permits much higher spectral S/N ratios. Figure 4 compares the S/N ratios between spectra excited by the excimer and cw laser systems. The ordinates of these spectra are normalized to the incident excitation average power. The 1.05-mW, 100-Hz excimer laser output (10.5 μJ/pulse) was focused to a ~400-μm diameter at the sample. This was the smallest spot size that did not damage the quartz capillary sample holder. The cw laser had no similar limit; we found that we could focus the cw Ar$^+$-ion laser to a 68-μm spot size with a 7-cm-focal-length lens. The low-power cw laser at 1.2 mW focused into a 68-μm spot

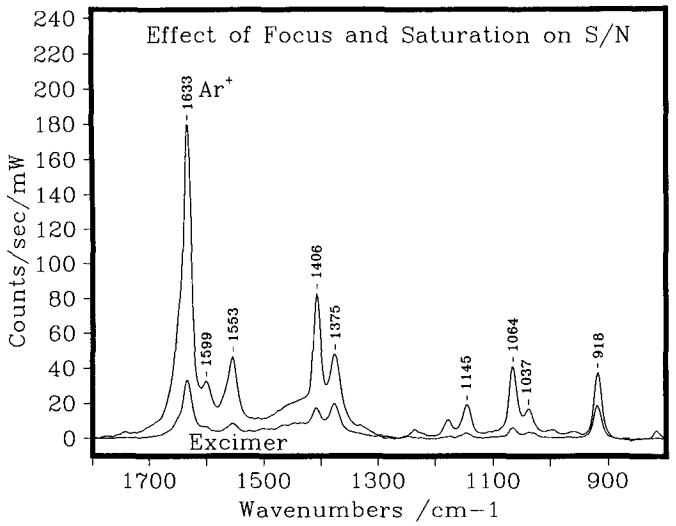

FIG. 4. Comparison between spectral signal-to-noise ratios of 244-nm excited spectra of pyrene in acetonitrile obtained with the pulsed excimer, compared to the cw Ar^+-ion laser. The excimer laser was focused to the smallest spot size that did not break the quartz sample capillary. Excimer laser: average power, 1.05 mW; spot size, ~382 μm; pulse energy flux, 9 mJ/cm²; pulse width, 16 ns, repetition rate, 100 Hz. Ar^+-ion laser: average power, 1.2 mW; spot size, 68 μm, power density at sample, ~33 W/cm²; spectral slit width, 100 μm; accumulation time, 100 s.

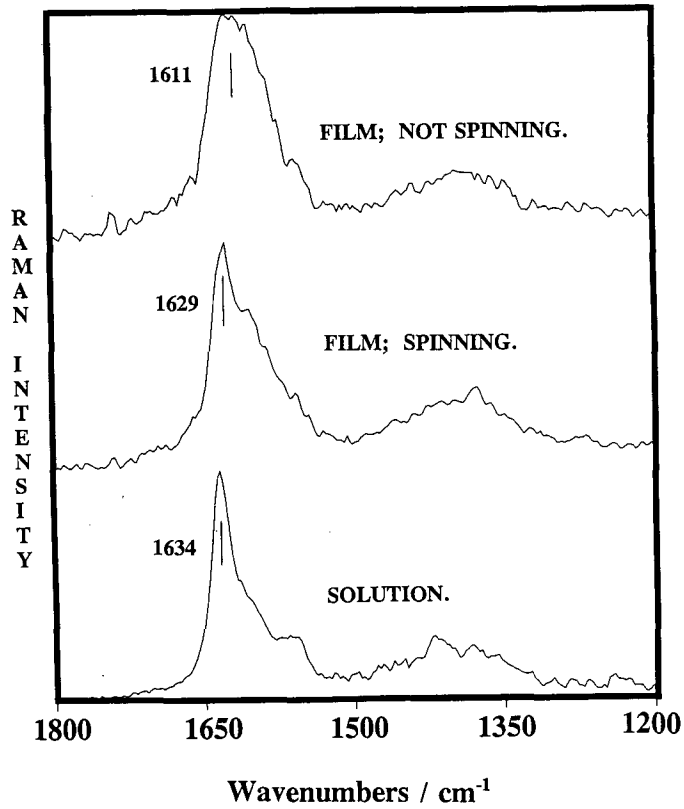

FIG. 5. UV resonance Raman spectra of a coal-liquid residue excited at 244 nm. Spot size at sample, 209 μm; average power, 10 mW; spectrograph resolution, 11 cm^{-1}; accumulation time, 1 min. (Top) Solid film of coal-liquid residue cast by evaporating tetrahydrofuran solution. Sample static. (Middle) Same as top spectrum, but sample is spinning in laser beam. (Bottom) Solution of 0.2 g/L coal-liquid residue dissolved in tetrahydrofuran, where the contribution of the tetrahydrofuran solvent has been subtracted off.

size shows an approximately sixfold increase of intensity per mW over that observed in the excimer-excited spectrum (spot size = ~400 μm). By comparing the pyrene intensities relative to the 918-cm^{-1} acetonitrile band intensity, we determined that approximately half the Fig. 4 intensity increase derives from the decreased pyrene saturation, while the remaining threefold increase derives from an increased signal throughput. We calculated that we should obtain a sixfold increase, but did not observe it, probably because of aberrations in the existing focusing and collection optics, which were designed for the diffusely focused pulsed laser. The increased signal intensity per incident mW results in an approximately 2.5-fold improved S/N ratio.

Figure 5 shows the ability of the cw Ar^+-ion laser source to obtain resonance Raman spectra of solid samples. Figure 5 shows a comparison of spectra of samples of coal-liquid residues created during a coal liquefaction reaction. The sample consists of the tetrahydrofuran soluble residuals which remain after all compounds are distilled off under vacuum. The Fig. 5 spectra (top and middle, respectively) are of a stationary and spinning solid film prepared by drying a tetrahydrofuran solution of the residuals on an aluminum block. All the spectra show a dominating peak between 1620 and 1640 cm^{-1}. The Fig. 5 stationary spectrum shows a broadened peak around 1620 cm^{-1}, which is shifted to lower frequency in comparison to the spinning sample (middle spectrum). We believe this broadening and shifting result from sample heating or from formation of long-lived excited species. Spinning the sample in the beam distributes the laser energy, and the spectrum closely resembles that of the same sample dissolved in tetrahydrofuran, in which it is completely soluble (Fig. 5, bottom spectrum). Essentially identical spectra can be obtained from the residues by packing the powder into a quartz capillary. All the 244-nm excited spectra show the dominating presence of a band at ~1630 cm^{-1} and broader features between 1300 and 1400 cm^{-1}, which result from ring-breathing motions of polycyclic aromatic hydrocarbon rings.[2-6] We are in the process of determining the species present in the coal-liquid residuals. The importance of the data shown here is the fact that the cw laser makes it possible, for the first time, to study the UV Raman spectra of solid absorbing samples. The steady-state temperature rise which occurs with the cw laser is much less than that with the pulsed laser; if the sample is spun, the temperature rise is negligible (<1 K), and the samples do not thermally decompose. Thus, solid samples can be studied as packed powders with essentially no sample preparation.

Figure 6 shows the importance of the high S/N spectra for studying the structure and environment of polycyclic aromatic hydrocarbons intercalated into DNA. Figure 6B shows the UV resonance Raman spectrum of a sample of calf thymus DNA with one pyrene intercalated for every 70 base pairs. The DNA nucleic acid bands are shaded in this spectrum. Upon addition of the detergent sodium dodecylsufate (SDS), the pyrene is extracted into SDS micelles. Spectrum 6A shows the increased intensity which occurs for the pyrene bands upon extraction from the DNA; the excitonic interactions between the pyrene and the DNA bases cause a large absorption and Raman hypochromism.[15c]

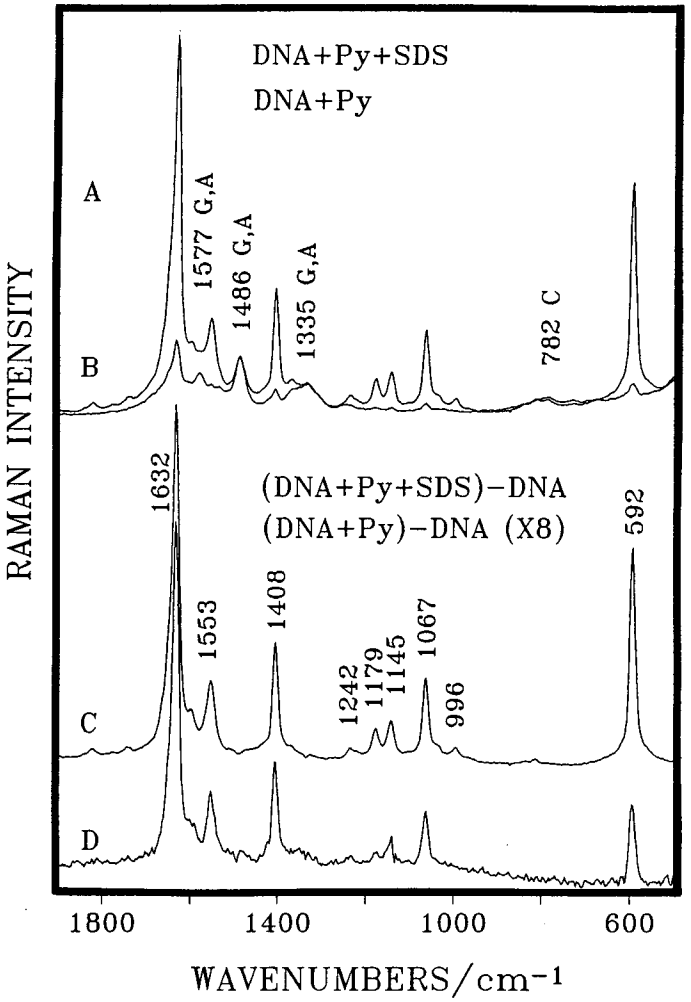

FIG. 6. UV resonance Raman spectra of pyrene and calf thymus DNA. Concentration of DNA nucleic acid bases, 2.3 mM. Pyrene, 33 μM. SDS, 1% by wt. Excitation at 244 nm with cw Ar^+-ion laser. Power density, 15 W/cm². Sample accumulation time, 10 min. Spectrograph slit width, 100 μm. (*A*) sample contains DNA, pyrene and SDS. (*B*) sample from *A* but before addition of SDS. Difference spectra: (*C*) Spectrum *A* minus spectrum of pure calf thymus DNA. (*D*) Spectrum *B* minus spectrum of pure calf thymus DNA.

The spectra have very high S/N; thus, it is possible to obtain difference spectra which display the Raman spectra of pyrene in the micelles (Fig. 6C) and the pyrene intercalated into the DNA (Fig. 6D). It is evident from these spectra that the relative intensities of the 592- and 1632-cm^{-1} bands significantly differ. This observation results from the differences in the absorption band line shape and the peak wavelength for pyrene in the micelles compared to that in the DNA, combined with the fact that the bandwidths of the Raman excitation profiles differ for these two bands. The high S/N ratios allow us to examine intercalation of PAHs and aromatic drugs within DNA. Because of the cw excitation, the spectra are not confounded by saturation.

Figure 7 shows the UV resonance Raman spectrum of human methemoglobin fluoride excited at 228.5 nm. This excitation wavelength is almost ideal for resonance Raman enhancement of tyr and trp residues in proteins, since the Raman excitation profile maximum is red shifted in comparison to the absorption of these amino acids in aqueous solution. The 244-nm excitation wavelength

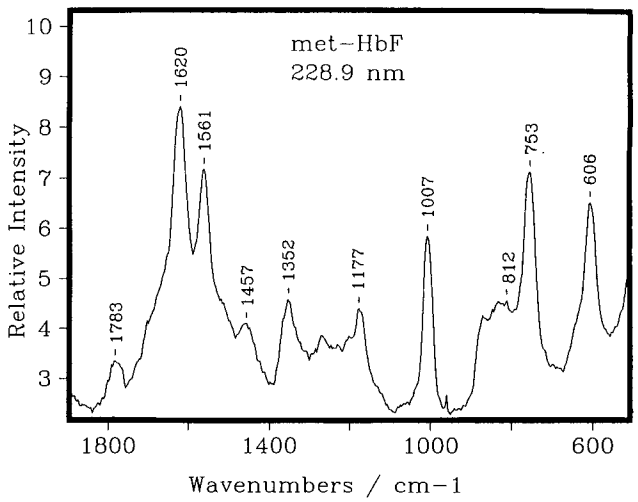

FIG. 7. UV resonance Raman spectrum excited at 228.5 nm of human methemoglobin fluoride. Hemoglobin concentration, 70 μM in heme; NaF concentration, 0.1 M; Cacodylate buffer was used as an internal standard at 0.1 M concentration. The 605-cm^{-1} band results from the cacodylate. Power flux, 6 mW. Laser spot size, 0.7 mm; Accumulation time, 10 min; spectrograph slit width, 200 μm.

would be ideal for studies of tyrosinate. The S/N ratios are sufficiently high for it to be possible to monitor small differences in protein quaternary structure, as the quaternary protein structure is modified by addition of allosteric effectors such as inositol hexaphosphate.

CONCLUSIONS

We have demonstrated the utility of a new cw Ar^+-ion UV laser source for Raman spectral measurements. This new intracavity doubled Ar^+-ion laser has five lines below 260 nm with sufficient powers for Raman measurements. The cw nature of the excitation avoids nonlinear sample photochemistry, sample thermal degradation, and ground-state saturation. The beam can be focused to a small sample volume which can be efficiently collected by the Raman spectrometer; this capability results in very high spectral S/N ratios. This new laser permits the use of colored solid samples. The only disadvantage of this laser is that it is not completely tunable. However, future intracavity doubling of Kr^+-ion lasers, for example, should add additional discrete lines. This laser is less expensive and is easier to use than the previous YAG-based and excimer-based systems. Another major advantage of this laser is that it will now permit us to build a UV Raman microscope to begin the examination of microscopic samples such as single cells and organelles.

ACKNOWLEDGMENTS

We gratefully acknowledge support from NIH Grants 1R01 30741-11 and R03 RR05502 (to S.A.A.). In addition, we gratefully acknowledge partial support for funding of the laser from the University of Pittsburgh Materials Research Center, through funding from the Air Force Office of Scientific Research.

1. (a) S. A. Asher, Ann. Rev. Phys. Chem. **39,** 537 (1988); S. A. Asher, Anal. Chem. **65,** 59A (1993), and S. A. Asher, Anal. Chem. **65,** 201A (1993). (b) I. Harada and H. Takeuchi, in *Spectroscopy of Biological Systems,* R. T. Clark and R. E. Hester, Eds. (J. Wiley and

Sons, New York, 1986). (c) B. Hudson and L. Mayne, Meth. Enzym. **130,** 331 (1986). (d) B. Hudson, Spectroscopy **1,** 22 (1986).
2. C. M. Jones and S. A. Asher, J. Chem. Phys. **89,** 2649 (1988).
3. S. A. Asher, Anal. Chem. **56,** 720 (1984).
4. C. M. Jones, T. A. Naim, M. Ludwig, J. Murtaugh, P. F. Flaugh, J. M. Dudik, C. R. Johnson, and S. A. Asher, Trends Anal. Chem. **4,** 75 (1985).
5. C. R. Johnson and S. A. Asher, Anal. Chem. **56,** 2258 (1984).
6. (a) S. A. Asher and C. M. Jones, in *New Applications of Analytical Techniques to Fossil Fuels,* ACS Symposium Series, M. Perry and H. Retcofsky, Eds. (American Chemical Society, Washington, D.C., 1986), Vol. 31, p. 170. (b) R. Rummelfanger, S. A. Asher, and M. B. Perry, Appl. Spectrosc. **42,** 267 (1988).
7. (a) S. A. Asher, C. R. Johnson, and J. Murtaugh, Rev. Sci. Instr. **54,** 1657 (1983). (b) M. Jones, V. L. Devito, P. A. Harmon, and S. A. Asher, Appl. Spectrosc. **41,** 1268 (1987).
8. L. D. Ziegler and B. Hudson, J. Chem. Phys. **74,** 989 (1981).
9. C. R. Johnson, M. Ludwig, S. O'Donnell, and S. A. Asher, J. Am. Chem. Soc. **106,** 5008 (1984).
10. (a) C. R. Johnson, M. Ludwig, and S. A. Asher, J. Am. Chem. Soc. **108,** 905 (1986). (b) M. Ludwig and S. A. Asher, J. Am. Chem. Soc. **110,** 1005 (1988). (c) J. Sweeney and S. A. Asher, J. Phys. Chem. **94,** 4784 (1990).
11. (a) J. M. Dudik, C. R. Johnson, and S. A. Asher, J. Chem. Phys. **82,** 1732 (1985). (b) S. A. Asher, P. J. Larkin, and J. Teraoka, Biochemistry **30,** 5944 (1991).
12. (a) J. Sweeney and S. A. Asher, J. Phys. Chem. **94,** 4784 (1990). (b) J. Sweeney, P. A. Harmon, S. A. Asher, C. M. Hutnik, and A. G. Szabo, J. Am. Chem. Soc. **113,** 7531 (1991).
13. (a) T. G. Spiro, G. Smulevich, and C. Su, Biochemistry **29,** 4497 (1990). (b) R. Rava and T. G. Spiro, J. Phys. Chem. **89,** 1856 (1985). (c) J. B. Ames, S. R. Bolton, N. M. Netto, and R. A. Mathies, J. Am. Chem. Soc. **112,** 9007 (1990). (d) I. Harada, T. Yamagishi, K. Uchida, and H. Takeuchi, J. Am. Chem. Soc. **112,** 2443 (1990). (e) M. N. Netto, S. P. Fodor, and R. A. Mathies, Protochem. Photobiol. **52,** 605 (1990).
14. (a) R. P. Rava and T. G. Spiro, Biochemistry **24,** 1861 (1985). (b) K. R. Rodgers, C. Su, S. Subramaniam, and T. G. Spiro, J. Am. Chem. Soc. **114,** 3697 (1992). (c) S. Kaminaka and T. Kitagawa, J. Am. Chem. Soc. **114,** 3256 (1992). (d) S. Kaminaka, T. Ogura, and T. Kitagawa, J. Am. Chem. Soc. **112,** 23 (1990). (e) C. Su, Y. D. Park, G. Y. Liu, and T. G. Spiro, J. Am. Chem. Soc. **111,** 3457 (1989).
15. (a) R. G. Efremov, A. V. Feofanov, K. N. Dzhandzhugazyan, N. N. Modyanov, and I. R. Nabiev, FEBS Lett. **260,** 257 (1990). (b) J. R. Perno, C. A. Grygon, and T. G. Spiro, J. Phys. Chem. **93,** 5672 (1989). (c) S. P. A. Fodor and T. G. Spiro, J. Am. Chem. Soc. **108,** 3198 (1986). (d) W. L. Kubasek, B. Hudson, and W. Peticolas, Proc. Natl. Acad. Sci. USA **82,** 2369 (1985). (e) K. Bajdor, Y. Nishimura, and W. L. Peticolas, J. Am. Chem. Soc. **109,** 3514 (1987). (f) N. Cho and S. A. Asher, J. Am. Chem. Soc., in preparation (1992).
16. (a) Y. P. Zhang and L. D. Ziegler, J. Phys. Chem. **93,** 6665 (1989). (b) L. D. Ziegler, J. Chem. Phys. **86,** 1703 (1987). (c) D. L. Phillips and A. B. Myers, J. Chem. Phys. **95,** 226 (1991). (d) B. Li and A. B. Myers, J. Chem. Phys. **94,** 2458 (1991).
17. (a) S. A. Asher and C. R. Johnson, J. Phys. Chem. **89,** 1375 (1985). (b) S. A. Asher and J. L. Murtaugh, Appl. Spectrosc. **42,** 83 (1988). (c) P. A. Harmon and S. A. Asher, J. Chem. Phys. **88,** 2925 (1988).
18. J. M. Dudik, C. R. Johnson, and S. A. Asher, J. Phys. Chem. **89,** 3805 (1985).
19. (a) S. Song, S. A. Asher, S. Krimm, and K. D. Shaw, J. Am. Chem. Soc. **113,** 1155 (1991). (b) S. Krimm, S. Song, and S. A. Asher, J. Am. Chem. Soc. **111,** 4290 (1989). (c) S. Song, S. A. Asher, S. Krimm, and J. Bandekar, J. Am. Chem. Soc. **110,** 8547 (1988).
20. (a) L. C. Mayne, L. D. Ziegler, and B. Hudson, J. Phys. Chem. **89,** 3395 (1985). (b) L. C. Mayne and B. Hudson, J. Phys. Chem. **95,** 2962 (1991). (c) B. S. Hudson and L. C. Mayne, in *Biological Applications of Raman Spectroscopy,* T. G. Spiro, Ed. (John Wiley, New York, 1987), Vol. II.
21. (a) Y. Wang, R. Purrello, T. Jordan, and T. G. Spiro, J. Am. Chem. Soc. **111,** 8274 (1989). (b) Y. Wang, R. Purrello, T. Jordan, and T. G. Spiro, J. Am. Chem. Soc. **113,** 6359 (1991). (c) Y. Wang, R. Purrello, S. Georgiou, and T. G. Spiro, J. Am. Chem. Soc. **113,** 6368 (1991). (d) S. Song and S. A. Asher, J. Am. Chem. Soc. **111,** 4295 (1989).
22. K. P. J. Williams and D. Klenerman, J. Raman Spectrosc. **23,** 191 (1992).
23. P. M. Killough, V. L. DeVito, and S. A. Asher, Appl. Spectrosc. **45,** 1067 (1991).
24. S. A. Asher and C. R. Johnson, Science **225,** 311 (1984).
25. J. Teraoka, P. A. Harmon, and S. A. Asher, J. Am. Chem. Soc. **112,** 2892 (1990).
26. P. A. Harmon, J. Teraoka, and S. A. Asher, J. Am. Chem. Soc. **112,** 8789 (1990).
27. S. A. Asher, Appl. Spectrosc. **38,** 276 (1984).
28. T. L. Gustafson, Optics Comm. **67,** 53 (1988).